2005-09-01

Impact of receive amplifier signal coupling on MIMO system performance

Michael A. Jensen
jensen@byu.edu

Matthew L. Morris

Original Publication Citation

Morris, M. L., and M. A. Jensen. "Impact of Receive Amplifier Signal Coupling on MIMO System Performance." Vehicular Technology, IEEE Transactions on 54.5 (25): 1678-83

Impact of Receive Amplifier Signal Coupling on MIMO System Performance

Matthew L. Morris and Michael A. Jensen, *Senior Member, IEEE*

***Abstract*—This paper uses a detailed model of multiple input multiple output (MIMO) systems to explore the impact of signal coupling in the receiver front end on communication capacity. The model is applied to assess the performance of a MIMO system with two transmit and receive antennas in a simulated multipath environment for different amplifier coupling levels. The results show that in practical scenarios where simple impedance matching techniques are used, the circuit coupling can reduce the signal-to-noise ratio at the receiver and therefore degrade the achievable MIMO capacity.**

***Index Terms*—Amplifier noise, coupled circuits, electromagnetic coupling, multiple input multiple output (MIMO) systems.**

I. Introduction

A FLURRY of recent activity has demonstrated the impact of electromagnetic coupling in the transmit and receive antenna arrays on the potential performance of multiple input multiple output (MIMO) communication systems [1]–[5]. These studies have clearly shown that unless very sophisticated (and likely costly) impedance matching networks are realized to connect the antennas to the transmit and receive electronics, this antenna coupling tends to reduce the system capacity. This understanding facilitates effective decision making regarding the tradeoff between antenna system complexity and overall system performance.

While these antenna coupling studies have provided a powerful framework for analysis of MIMO systems, they have neglected a second important coupling phenomenon—that of electromagnetic signal coupling in the radio receiver front end. As adoption of MIMO technology increases, there will be increased desire to integrate multiple receiver front ends on a single chip, particularly for mobile equipment. As this integration occurs, circuit level signal coupling will increase, potentially leading to altered signal correlation characteristics and signal-to-noise ratio (SNR) at the front end amplifier outputs. It is important to be able to quantify the impact of this coupling on the overall system performance to facilitate design decisions at the circuit level.

The goal of this work is to expand a previously developed MIMO system modeling framework to allow assessment of the performance degradations created by coupling in the receiver front end amplifiers [5], [6]. This approach develops the transfer matrix relation between the signals input to the transmit antenna terminals and the noisy signals observed at the receive amplifier outputs, and then uses this relation to formulate the MIMO system capacity. Coupled amplifiers are modeled using a simple yet flexible equivalent circuit. The formulation is applied to the simple case of a MIMO system with two transmit and receive antennas, with propagation conditions simulated using a multipath channel model. The results of these simulations reveal that the use of practical matching networks can lead to significant capacity degradation as the circuit coupling increases.

Manuscript received September 14, 2004; revised February 17, 2005. This work was supported by the National Science Foundation under Information Technology Research Grant CCR-0313056. The review of this paper was coordinated by Prof. R. Heath.

The authors are with the Department of Electrical and Computer Engineering, 459 Clyde Building, Brigham Young University, Provo, UT 84602 (e-mail: morris@ee.byu.edu; jensen@ee.byu.edu).

Digital Object Identifier 10.1109/TVT.2005.853467

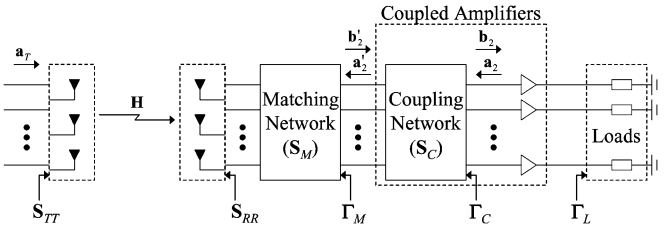

Fig. 1. Block diagram of the MIMO receiver front end with matching and amplifier coupling networks.

II. MIMO System Model

Characterizing a complete MIMO communication system requires a model that includes the antenna arrays, multipath propagation channel, receiver front end matching network, coupled receiver amplifiers, and amplifier load terminations. Fig. 1 shows a block diagram of this system model. In this diagram and throughout the analysis, boldface uppercase and lowercase letters will describe matrices and column vectors, respectively, with H_{mn} denoting the element occupying the mth row and nth column of the matrix $\mathbf{H}$, and h_m representing the mth element of the vector $\mathbf{h}$. We use scattering parameters (S-parameters) referenced to a real impedance Z_0 [7] to describe the signal flow within the network wherein the input and output waves are denoted as $\mathbf{a}$ and $\mathbf{b}$, respectively.

In Fig. 1, $\mathbf{S}_{TT}$ and $\mathbf{S}_{RR}$ represent the S-parameter matrices (or S-matrices) of the transmit and receive antenna arrays, respectively. These can, in general, be full matrices which include the mutual impedance created by electromagnetic antenna mutual coupling. The various values of $\mathbf{\Gamma}$ in the block diagram represent multiport (matrix) reflection coefficients observed at the locations indicated. Also, the propagation channel matrix $\mathbf{H}$ relates the open circuit voltages on the receive antennas to the excitation currents on the transmit antennas.

The coupled amplifier model used in this analysis consists of a passive coupling network followed by uncoupled, noisy amplifiers as shown in Fig. 1. It is noteworthy that a general coupled

amplifier model will likely include a coupling network after the noisy amplifiers as well. However, the formulations in [6] reveal that, practically speaking, MIMO system capacity is determined by the receiver system components placed *before* the point of amplifier noise injection. This observation is expected, since any *fixed* linear transformation (i.e., a transformation that does not adapt to the specific signal and noise characteristics) occurring after the point of noise injection will have the same impact on the signal as it does on the noise, and therefore will not change the system SNR. Therefore, inclusion of coupling effects at the amplifier output will not impact the capacity results, justifying the simplified model considered here.

The matching network, amplifier coupling network, and uncoupled amplifier blocks in the receiver are described by block matrix S-parameter representations $\mathbf{S}_M, \mathbf{S}_C$, and $\mathbf{S}_A$, respectively, that assume the form

$$\mathbf{S}_P = \begin{bmatrix} \mathbf{S}_{P,11} & \mathbf{S}_{P,12} \\ \mathbf{S}_{P,21} & \mathbf{S}_{P,22} \end{bmatrix} \tag{1}$$

where $P \in \{M, C, A\}$, and 1 and 2 refer to the network input and output ports, respectively.

A. Signal Model

The developments in [6] provide a relatively lengthy S-parameter analysis to relate the vector $\mathbf{v}_L$ of voltages at the amplifier terminations to the vector $\mathbf{a}_T$ of input voltage waves at the transmitter when no coupling exists in the amplifier ($\mathbf{S}_C = \mathbf{I}$, where $\mathbf{I}$ is the identity matrix). We can effectively use the results of this analysis to simplify the derivation for the case where the amplifier coupling network is included. Specifically, when the coupling network is removed, the signal model relating the vector of voltages at the amplifier terminations to the vector of input voltage waves at the transmit antenna terminals is given by

$$\mathbf{v}_L = \mathbf{Q}[\mathbf{G}_M \mathbf{S}_{RT} \mathbf{a}_T + \mathbf{\Gamma}_M \mathbf{b}_\eta - \mathbf{a}_\eta] \tag{2}$$

where

$$\mathbf{S}_{RT} = (\mathbf{I} - \mathbf{S}_{RR})\mathbf{H}(\mathbf{I} - \mathbf{S}_{TT}) \tag{3}$$

$$\mathbf{G}_M = \mathbf{S}_{M,21}(\mathbf{I} - \mathbf{S}_{RR}\mathbf{S}_{M,11})^{-1} \tag{4}$$

$$\mathbf{\Gamma}_M = \mathbf{S}_{M,22} + \mathbf{G}_M \mathbf{S}_{RR} \mathbf{S}_{M,12} \tag{5}$$

$$\mathbf{Q} = Z_0^{1/2}(\mathbf{I} + \mathbf{\Gamma}_L)\left[(\mathbf{I} - \mathbf{\Gamma}_M \mathbf{S}_{A,11})\mathbf{S}_{A,21}^{-1} \times (\mathbf{I} - \mathbf{S}_{A,22}\mathbf{\Gamma}_L) - \mathbf{\Gamma}_M \mathbf{S}_{A,12}\mathbf{\Gamma}_L\right]^{-1}. \tag{6}$$

The voltage wave vectors $\mathbf{a}_\eta$ and $\mathbf{b}_\eta$ represent the forward and reverse traveling noise voltages generated by the noisy amplifiers. The statistical characteristics of these noise waves can be obtained from traditional device noise parameters as outlined in [6]. From the results in [6], we also obtain the relationship

$$\mathbf{b}_2' = \mathbf{G}_M \mathbf{S}_{RT} \mathbf{a}_T + \mathbf{\Gamma}_M \mathbf{a}_2'. \tag{7}$$

Our goal is now to use this result to develop the transfer function equivalent to (2) for the case when the coupling network is included. Substituting $\mathbf{a}_2' = \mathbf{S}_{C,11}\mathbf{b}_2' + \mathbf{S}_{C,12}\mathbf{a}_2$ into (7) and rearranging the result leads to

$$\mathbf{b}_2' = (\mathbf{I} - \mathbf{\Gamma}_M \mathbf{S}_{C,11})^{-1}(\mathbf{G}_M \mathbf{S}_{RT}\mathbf{a}_T + \mathbf{\Gamma}_M \mathbf{S}_{C,12}\mathbf{a}_2). \tag{8}$$

Finally, substitution of (8) into the equation $\mathbf{b}_2 = \mathbf{S}_{C,21}\mathbf{b}_2' + \mathbf{S}_{C,22}\mathbf{a}_2$ produces

$$\mathbf{b}_2 = \mathbf{G}_C \mathbf{G}_M \mathbf{S}_{RT} \mathbf{a}_T + \mathbf{\Gamma}_C \mathbf{a}_2 \tag{9}$$

where

$$\mathbf{G}_C = \mathbf{S}_{C,21}(\mathbf{I} - \mathbf{\Gamma}_M \mathbf{S}_{C,11})^{-1} \tag{10}$$

$$\mathbf{\Gamma}_C = \mathbf{S}_{C,22} + \mathbf{G}_C \mathbf{\Gamma}_M \mathbf{S}_{C,12}. \tag{11}$$

Equations (7) and (9) relate the forward and reverse traveling waves at the uncoupled amplifier input ports for the cases when the amplifier coupling network is excluded and included, respectively. Other than the differences in these two expressions, the remainder of the analysis required to obtain the complete transfer relationship for the two systems is identical. Therefore, comparing these two equations, we observe that when the coupling is included, we must replace $\mathbf{G}_M$ by the product $\mathbf{G}_C\mathbf{G}_M$ and the reflection coefficient $\mathbf{\Gamma}_M$ by the reflection coefficient $\mathbf{\Gamma}_C$. Using these observations in (2) leads to the signal model for the case when amplifier coupling is included given by

$$\mathbf{v}_L = \mathbf{Q}_0[\mathbf{H}_0 \mathbf{a}_T + \boldsymbol{\eta}] \tag{12}$$

where

$$\mathbf{H}_0 = \mathbf{G}_C \mathbf{G}_M \mathbf{S}_{RT} \tag{13}$$

$$\boldsymbol{\eta} = \mathbf{\Gamma}_C \mathbf{b}_\eta - \mathbf{a}_\eta \tag{14}$$

and $\mathbf{Q}_0$ results from (12) with $\mathbf{\Gamma}_M$ replaced by $\mathbf{\Gamma}_C$.

The matrix $\mathbf{Q}_0$ in (12) is a complex function of the network parameters. However, as shown in [6], since $\mathbf{Q}_0$ multiplies both the signal and the noise it does not impact the system capacity, and therefore will not be of concern in this development. Therefore, we can consider the relevant output signal as $\mathbf{y} = \mathbf{Q}_0^{-1}\mathbf{v}_L$ to obtain the simplified signal model

$$\mathbf{y} = \mathbf{H}_0 \mathbf{a}_T + \boldsymbol{\eta}. \tag{15}$$

Since the impact of all network components placed after the amplifier appears in $\mathbf{Q}_0$, this confirms the validity of the simplified model where we ignore post-amplifier coupling effects for the purpose of computing capacity.

B. Capacity

Using the signal model of (15), it is straightforward to compute the capacity of the MIMO system. We will assume that the transmitter is informed concerning the channel state information, leading to a capacity that can be obtained from the waterfilling solution [8]. In computing this capacity, however, we must properly formulate the covariance of the noise vector $\boldsymbol{\eta}$ using the statistical properties of the noise waves $\mathbf{a}_\eta$ and $\mathbf{b}_\eta$. As outlined in [6] and [9], these noise waves can be represented as zero-mean Gaussian random variables, with noise in each amplifier uncorrelated with that of all other amplifiers. The relevant

covariances of the noise vectors are

$$\begin{aligned}\mathrm{E}\{\mathbf{a}_\eta \mathbf{a}_\eta^\dagger\} &= k_B T_\alpha B\mathbf{I}\\ \mathrm{E}\{\mathbf{b}_\eta \mathbf{b}_\eta^\dagger\} &= k_B T_\beta B\mathbf{I}\\ \mathrm{E}\{\mathbf{a}_\eta \mathbf{b}_\eta^\dagger\} &= k_B T_\Gamma^* B\mathbf{I},\end{aligned} \tag{16}$$

where k_B is the Boltzmann constant, B is the system noise power bandwidth, $\{\cdot\}^\dagger$ indicates a conjugate transpose, and $\mathrm{E}\{\cdot\}^\dagger$ is an expectation. The effective noise temperatures $(T_\alpha, T_\beta, T_\Gamma = T_\gamma e^{j\phi_\gamma})$ for the (assumed identical) amplifiers are readily computed from other noise parameters [9]. These results lead to a noise covariance of

$$\begin{aligned}\mathbf{R}_\eta &= \mathrm{E}\{\boldsymbol{\eta}\boldsymbol{\eta}^\dagger\}\\ &= k_B B \underbrace{(T_\alpha \mathbf{I} + T_\beta \boldsymbol{\Gamma}_C \boldsymbol{\Gamma}_C^\dagger - T_\Gamma \boldsymbol{\Gamma}_C - T_\Gamma^* \boldsymbol{\Gamma}_C^\dagger)}_{T_\alpha \mathbf{R}_{\eta o}}\end{aligned} \tag{17}$$

where we have factored out the constant T_α from $\mathbf{R}_{\eta o}$ so that the structure of $\mathbf{R}_{\eta o}$ is a function only of the relative values T_β/T_α and T_Γ/T_α. Using this representation, the absolute noise value controlled by $k_B B T_\alpha$ can be specified based on a desired SNR level. With this form of the noise covariance, the mutual information of $\mathbf{y}$ and $\mathbf{a}_T$ can be expressed as

$$I(\mathbf{y}, \mathbf{a}_T) = \log_2 \frac{|\mathbf{H}_0 \mathbf{R}_T \mathbf{H}_0^\dagger + \mathbf{R}_\eta|}{|\mathbf{R}_\eta|}, \tag{18}$$

where $\mathbf{R}_T = \mathrm{E}\{\mathbf{a}_T \mathbf{a}_T^\dagger\}$ is the covariance of the transmitted signal. Using the eigenvalue decomposition $\mathbf{R}_{\eta o} = \boldsymbol{\xi}_\eta \boldsymbol{\Lambda}_\eta \boldsymbol{\xi}_\eta^\dagger$ where $\boldsymbol{\xi}_\eta$ is unitary, the mutual information expression can be rearranged to the form

$$I(\mathbf{y}, \mathbf{a}_T) = \log_2 \left| \frac{\mathbf{Z}\mathbf{R}_T \mathbf{Z}^\dagger}{k_B B T_\alpha} + \mathbf{I} \right|, \tag{19}$$

where $\mathbf{Z} = \boldsymbol{\Lambda}_\eta^{-1/2} \boldsymbol{\xi}_\eta^\dagger \mathbf{H}_0$. The capacity results when the transmit covariance matrix $\mathbf{R}_T$ is specified according to the water filling solution, with the total transmit power limited according to $\mathrm{Tr}(\mathbf{R}_T) \le P_T$. This is a detailed yet well known derivation, and details can be found in [8], [10].

C. Matching Network Specification

The effective channel response matrix $\mathbf{H}_0$ in (13) depends on the S-parameter matrix $\mathbf{S}_M$ describing the matching network connecting the receive antenna to the coupled amplifiers. We must therefore specify this matching network response to evaluate the MIMO system capacity. In practical high-frequency amplifier design, the behavior of the amplifier depends on the source termination observed by the active amplifier device. For example, this source termination can be chosen to achieve either minimum amplifier noise figure or maximum signal power transfer. Determining these optimal source terminations is routinely performed for high frequency active devices used in receiver front ends [11].

In this analysis, we assume that we know the appropriate amplifier source terminations to achieve a desired design goal for the uncoupled amplifiers. This knowledge then allows specification of the diagonal matrix $\boldsymbol{\Gamma}_C$. For example, if Γ_{opt} is the amplifier source termination for minimum noise figure, $\boldsymbol{\Gamma}_C = \Gamma_{\mathrm{opt}}\mathbf{I}$.

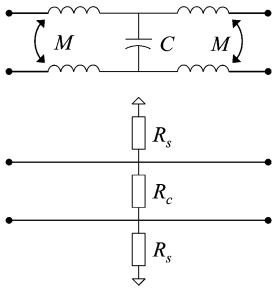

Fig. 2. Four-port networks used to model amplifier coupling for a two-antenna MIMO receiver when coupling is due to electromagnetic effects (top) and substrate effects (bottom).

Then, (11) can be rearranged to the form

$$\begin{aligned}\boldsymbol{\Gamma}_M = {} & \mathbf{S}_{C,21}^{-1}(\boldsymbol{\Gamma}_C - \mathbf{S}_{C,22})\\ & \times \left[\mathbf{S}_{C,12} + \mathbf{S}_{C,11}\mathbf{S}_{C,21}^{-1}(\boldsymbol{\Gamma}_C - \mathbf{S}_{C,22})\right]^{-1}.\end{aligned} \tag{20}$$

Simply stated, we have used our knowledge of the desired amplifier source terminations to specify the appropriate value of $\boldsymbol{\Gamma}_M$. With $\boldsymbol{\Gamma}_M$ known, the techniques developed in [6] can be used to construct the matching network S-parameter matrix $\mathbf{S}_M$ which achieves the desired matching condition.

D. Amplifier Coupling Network

Within the receiver model framework, we must develop a simple yet flexible model for the amplifier coupling network that can be used to determine $\mathbf{S}_C$. To facilitate drawing conclusions about the impact of coupling on MIMO system performance, we will focus on a MIMO architecture with two antennas at transmit and receive, leading to a coupling network with two input and two output ports.

Naturally, any level of sophistication in the coupling network can be accommodated by the framework provided that its S-matrix $\mathbf{S}_C$ can be constructed. To facilitate assessment of how the physical mechanisms impact capacity, we will focus on two simple coupling networks that model different coupling effects and whose symmetry allows simple construction of $\mathbf{S}_C$ [7]. First, electromagnetic coupling between input transmission lines or bond wires [12] can be simply modeled using the top architecture in Fig. 2. This network includes mutual inductance M and capacitance C which we will normalize as $M_0 = \omega M/Z_0$ and $C_0 = \omega C Z_0$, where ω is the operation radian frequency. Coupling through the substrate [13] can be effectively modeled using a resistance R_c between the amplifiers as well as resistances R_s to ground, as shown in the bottom architecture in Fig. 2 [14]. In this case, the range of coupling resistances over which the desired amplifier source termination $\boldsymbol{\Gamma}_C$ can be realized may be limited since the fixed resistances may require the matching network to produce negative output resistances. This can be assessed by ensuring that no eigenvalues of $\boldsymbol{\Gamma}_M$ have a magnitude greater than unity. In the example computations used here, the resistances lie within a practical range where this condition does not occur.

We will discuss the system capacity in reference to the level of coupling created by the amplifier coupling network. This coupling level will be quantified by driving one of the input ports with all other ports terminated in Z_0. The coupling coefficient κ represents the ratio of the power exiting the coupled output port to the sum of the powers exiting both output ports.

III. Computational Examples

For the following simulations, we assume the transmit and receive arrays consist of two uncoupled half wave dipole antennas with half wavelength spacing. The dipole impedance and radiation pattern are computed using closed form expressions [15]. The device used as a basis for the amplifier is a BJT taken from a Hewlett-Packard Application Note [16].

While the mathematical analysis can incorporate the effects of antenna mutual coupling (by making $\mathbf{S}_{TT}$ and $\mathbf{S}_{RR}$ full matrices), a detailed treatment of the capacity for coupled dipoles has been given in [6]. We therefore neglect antenna coupling here to allow observation of the impact of circuit-level coupling on the capacity. Naturally, a full simulation should include the impact of both phenomena using the framework developed. Which of these two factors will play the largest role in determining the ultimate MIMO performance will be a function of the antenna and circuit properties. We also point out that antenna and circuit coupling both produce the same type of effect on the system. The power of the framework outlined here is that it allows both coupling phenomena to be modeled in a physically meaningful way and does not simply lump the effects into generalized characteristics (such as signal correlation).

For all simulations, 1000 realizations of a path based channel model [17] are used to create a set of transfer matrices $\mathbf{H}$. Details on the implementation of this model, including the parameters used to model an indoor propagation environment, can be found in [18]. Because each realization of $\mathbf{H}$ has a unique average channel power gain (i.e., a unique Frobenius norm), we will set the additive noise level for each channel realization such that all realizations will have the same average single-input single-output (SISO) SNR. To accomplish this, for each channel realization we place single dipoles in the transmit and receive spaces and create a lossless receive matching network with $S_{M,11} = S_{RR}^*$ so that $\Gamma_M = 0$ (all terms are scalars, and $\mathbf{S}_C = \mathbf{I}$). We then can simplify the SISO SNR as

$$\mathrm{SNR}_S = \frac{|S_{RT}|^2}{1 - |S_{RR}|^2} \frac{P_T}{k_B B T_\alpha} \tag{21}$$

where P_T is the total transmit power. This SNR value is then averaged by moving each dipole in $0.1\ \lambda$ steps over a linear range of $1.5\ \lambda$. For a given transmit power, the value of $k_B B T_\alpha$ can be computed to achieve an average SISO SNR (20 dB in this work) for the channel realization.

Several matching networks will be used in the simulations, with the goal of all being minimum amplifier noise figure. First, we assume that we know $\mathbf{S}_C$ and wish to compensate for the coupling by creating a matching network that presents the optimal value of $\mathbf{\Gamma}_C$ to the amplifier. Note that $\mathbf{\Gamma}_C$ must be diagonal since we assume all amplifier coupling occurs in the coupling network. Therefore, this perfect matching network must, in general, be coupled ($\mathbf{S}_{M,ij}$ and $\mathbf{\Gamma}_M$ are full matrices), and therefore would be difficult to construct. However, this simulation provides an upper bound against which the performance of more practical matching approaches can be compared.

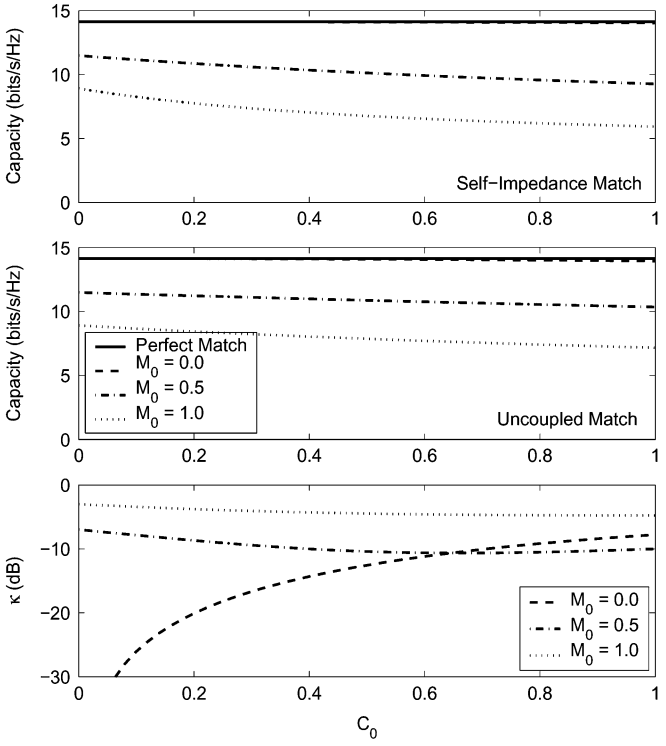

Fig. 3. Capacity for perfect and self-impedance matching (top plot), capacity for perfect and uncoupled matching (middle plot), and coupling coefficient as a function of amplifier coupling components C_0 and M_0.

We may also examine the system performance when using impedance matching networks that are more readily implemented in practice. For example, if we determine the value of $\mathbf{\Gamma}_M$ to provide the optimal $\mathbf{\Gamma}_C$ as discussed above, we can convert the reflection coefficient $\mathbf{\Gamma}_M$ to the (full) impedance matrix

$$\mathbf{Z}_M = Z_0(\mathbf{I} + \mathbf{\Gamma}_M)(\mathbf{I} - \mathbf{\Gamma}_M)^{-1}. \tag{22}$$

We next form the diagonal matrix $\bar{\mathbf{Z}}_M$ containing the diagonal elements of the original $\mathbf{Z}_M$, and then compute the diagonal reflection coefficient matrix $\bar{\mathbf{\Gamma}}_M$ with elements $\bar{\Gamma}_{M,ii} = (\bar{Z}_{M,ii} - Z_0)/(\bar{Z}_{M,ii} + Z_0)$. We can then construct the self impedance matching network to achieve this uncoupled diagonal reflection coefficient matrix. Finally, if we assume that we don't know $\mathbf{S}_C$ for the coupling network, we can design a matching network that presents the optimal (diagonal) reflection coefficient $\mathbf{\Gamma}_M$ assuming that the coupling network is not present (equivalent to the optimal value of $\mathbf{\Gamma}_C$ discussed in the prior paragraph). We will refer to this as the uncoupled match.

Fig. 3 shows the capacity averaged over the 1000 channel realizations for the three different matching assumptions as well as the coupling coefficient κ as a function of C_0 and M_0 for the electromagnetic coupling model. Because the perfect match compensates for any amplifier coupling, the capacity

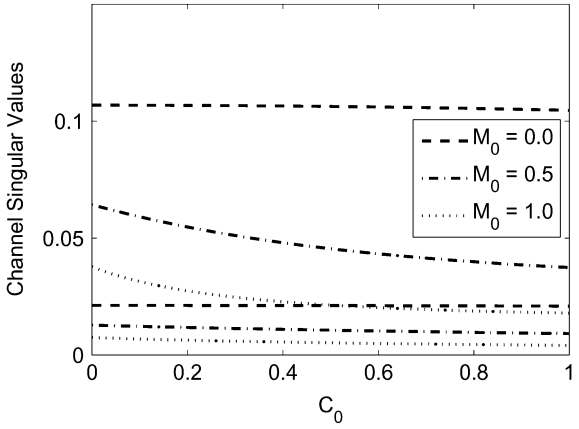

Fig. 4. Two singular values of the effective channel matrix as a function of the amplifier coupling components C_0 and M_0.

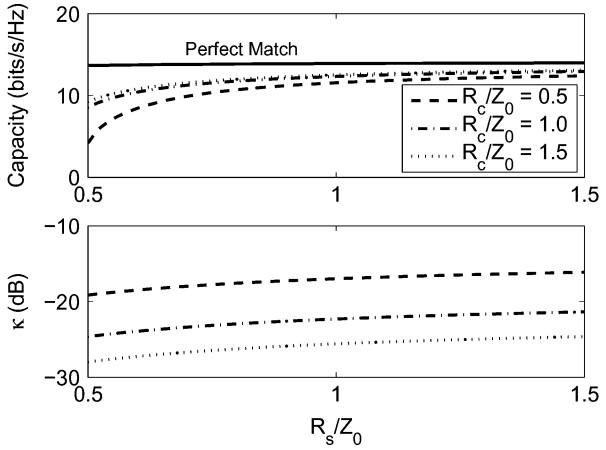

Fig. 5. Capacity for perfect and self-impedance matching and coupling coefficient for substrate coupling as a function of substrate resistances R_c/Z_0 and R_s/Z_0.

performance is independent of the coupling component values. In contrast, for the other matching networks, the performance degrades with increasing M_0 and C_0. One interesting feature of these results is that the capacity of the uncoupled match is slightly higher than that of the self impedance match. This occurs because the uncoupled match creates a value of $\mathbf{\Gamma}_0$ that is slightly better in terms of amplifier noise figure than the self-impedance match. However, this behavior is specific to the topology chosen, and which one of the two matching approaches is superior will depend on the actual system characteristics.

It is also interesting that while, generally speaking, the value of κ increases with increased C_0 and M_0, careful comparison reveals that the capacity is not closely tied to this coupling level. Most notably, the capacity for $M_0 = 0$ is always substantially higher than that for $M_0 = 0.5$, although the values of κ for these two inductance levels actually cross at moderate values of C_0. While the complexity of the system transfer function makes it difficult to provide an analytic expression from which the effect of amplifier coupling on capacity can be easily deduced, we can make some observations based on simulation. To accomplish this, we explore the behavior of the singular values of the effective channel matrix $\mathbf{H}_0$. These singular values represent the channel gains of the eigenchannels created by the propagation environment coupled with the antenna geometry and RF subsystem. For the 2×2 system under investigation here, the effect of coupling on these singular values can impact the capacity in two ways. First, if coupling creates a large imbalance between the singular values, capacity tends to decrease since the water filling solution concentrates most or all of the energy into the dominant eigenchannel. Second, power loss at the loads due to impedance mismatch created by the coupling (for the more practical matching network configurations) will reduce the received SNR and therefore system capacity.

Fig. 4 plots the two singular values for the system as a function of C_0 and M_0 for the case of the self-impedance match (similar results occur for the uncoupled match). As can be seen, coupling has only a minor impact on the relative values (ratio) of the singular values. In fact, careful analysis reveals that the ratio of the singular values gets smaller with increasing coupling component values, a trend that tends to improve the system capacity. However, this minor effect is overwhelmed by the large reduction in both singular values caused by the increased impedance mismatch associated with increased coupling (for the imperfect but practical matching network used here). As a result of this decreased signal strength, the capacity tends to decrease with increasing coupling component values. The key point to observe from this result is that it is not the signal coupling, but rather the reduced SNR created by imperfect power transfer through the system, which degrades the capacity performance.

Fig. 5 shows the capacity as well as the coupling coefficient for substrate coupling using the bottom architecture of Fig. 2 as a function of the normalized resistances R_c/Z_0 and R_s/Z_0. We once again observe that the capacity degradation is not strongly correlated with the coupling coefficient. Furthermore, examination of the singular values of $\mathbf{H}_0$ for this case again shows that the capacity decrease matches the fluctuations in the absolute levels of the singular values, reinforcing the observations drawn from the results for the electromagnetic coupling network discussed above. In this case, however, the effect is even more pronounced since the coupling network not only creates an impedance mismatch but also signal loss due to absorption in the resistances.

IV. Conclusion

This paper has used a detailed model to assess the performance of MIMO systems with signal coupling created in the receiver front end. The model has been applied to a MIMO system with two transmit and receive antennas with a simulated multipath environment for two different coupled amplifier models. The results have illustrated that for practical impedance matching networks, the coupling reduces the capacity due to the decreased power transfer created by the coupling induced mismatch. The framework presented could be used with any coupled amplifier model to assess the potential performance of other MIMO system implementations.

REFERENCES

[1] T. Svantesson and A. Ranheim, "Mutual coupling effects on the capacity of multielement antenna systems," in *Proc. 2001 IEEE Int. Conf. Acoustics, Speech, and Signal Processing*, vol. 4, Salt Lake City, UT, May 7–11, 2001, pp. 2485–2488.

[2] C. Waldschmidt, S. Schulteis, and W. Wiesbeck, "Complete RF system model for analysis of compact MIMO arrays," *IEEE Trans. Veh. Technol.*, vol. 53, pp. 579–586, May 2004.

[3] V. Jungnickel, V. Pohl, and C. von Helmolt, "Capacity of MIMO systems with closely spaced antennas," *IEEE Commun. Lett.*, vol. 7, pp. 361–363, Aug. 2003.

[4] P. N. Fletcher, M. Dean, and A. R. Nix, "Mutual coupling in multi-element array antennas and its influence on MIMO channel capacity," *Electron. Lett.*, vol. 39, pp. 342–344, Feb. 2003.

[5] J. W. Wallace and M. A. Jensen, "Mutual coupling in MIMO wireless systems: A rigorous network theory analysis," *IEEE Trans. Wireless Commun.*, vol. 3, pp. 1317–1325, Jul. 2004.

[6] M. L. Morris and M. A. Jensen, "Network model for MIMO systems with coupled antennas and noisy amplifiers," *IEEE Trans. Antennas Propag.*, vol. 53, pp. 545–552, Jan. 2005.

[7] D. M. Pozar, *Microwave Engineering*. New York: Wiley, 1998.

[8] G. G. Raleigh and J. M. Cioffi, "Spatio-temporal coding for wireless communication," *IEEE Trans. Commun.*, vol. 46, pp. 357–366, Mar. 1998.

[9] J. Engberg and T. Larsen, *Noise Theory of Linear and Nonlinear Circuits*. New York: Wiley, 1995.

[10] M. A. Khalighi, J. Brossier, G. Jourdain, and K. Raoof, "Water filling capacity of Rayleigh MIMO channels," in *Proc. 2001 IEEE 12th Int. Symp. Personal, Indoor and Mobile Radio Comm.*, vol. 1, San Diego, CA, Sep. 30–Oct. 3 2001, pp. 155–158.

[11] G. Gonzalez, *Microwave Transistor Amplifiers*. Englewood Cliffs, NJ: Prentice-Hall, 1997.

[12] R. E. Amaya, P. H. R. Popplewell, M. Cloutier, and C. Plett, "Analysis and measurements of EM and substrate coupling effects in common RF integrated circuits," in *Proc. 2004 IEEE Custom Integrated Circuits Conf.*, Orlando, FL, Oct. 3–6, 2004, pp. 363–366.

[13] W. Steiner, M. Pfost, H.-M. Rein, A. Stürmer, and A. Schüppen, "Methods for measurement and simulation of weak substrate coupling in high-speed bipolar ICs," *IEEE Trans. Microwave Theory Tech.*, vol. 50, pp. 1705–1713, Jul. 2002.

[14] R. Gharpurey and E. Charbon, "Substrate coupling: Modeling, simulation and design perspectives," in *Proc. 2004 5th Int. Symp. Quality Electronic Design*, San Jose, CA, Mar. 22–24, 2004, pp. 283–290.

[15] C. A. Balanis, *Antenna Theory: Analysis and Design*. New York: Wiley, 1997.

[16] "A low noise 4 GHz transistor amplifier using the HXTR-6101 silicon bipolar transistor," *Hewlett-Packard Application Note 967*, Palo Alto, CA: Hewlett-Packard Company, May, 1975.

[17] Q. H. Spencer, B. D. Jeffs, M. A. Jensen, and A. L. Swindlehurst, "Modeling the statistical time and angle of arrival characteristics of an indoor multipath channel," *IEEE J. Sel. Areas Commun.*, vol. 18, pp. 347–360, Mar. 2000.

[18] J. W. Wallace and M. A. Jensen, "Modeling the indoor MIMO wireless channel," *IEEE Trans. Antennas Propag.*, vol. 50, pp. 591–599, May 2002.

Matthew L. Morris received the B.S. degree in physics from Brigham Young University, Provo, UT, in 2000 and is currently working toward the Ph.D. degree in electrical engineering at the same university.

His research interests include multiple-input multiple-output communication with an emphasis on channel capacity.

Michael A. Jensen (S'93–M'95–SM'01) received the B.S. (summa cum laude) and M.S. degrees in electrical engineering from Brigham Young University (BYU), Provo, UT, in 1990 and 1991, respectively, and the Ph.D. in electrical engineering at the University of California, Los Angeles (UCLA) in 1994.

From 1989 to 1991 he was a Graduate Research Assistant in the Lasers and Optics Laboratory at BYU. In 1990 he received a National Science Foundation Graduate Fellowship. From 1991 to 1994, he was a Graduate Student Researcher in the Antenna Laboratory at UCLA. Since 1994, he has been at the Electrical and Computer Engineering Department at BYU where he is currently a Professor. His main research interests include antennas and propagation for personal communications, microwave circuit design, radar remote sensing, numerical electromagnetics, and optical fiber communications.

Dr. Jensen currently serves as a member of the Administrative Committee and the Joint Meetings Committee for the IEEE Antennas and Propagation Society and has served the society as Vice-Chair and Technical Program Chair for several symposia. He was awarded the H. A. Wheeler paper award in the IEEE Transactions on Antennas and Propagation in 2002, and best student paper award at the 1994 IEEE International Symposium on Antennas and Propagation. He is a member of Eta Kappa Nu and Tau Beta Pi.